Plasmacytoid dendritic cells initiate a complex chemokine and cytokine network and are a viable drug target in chronic HCV patients

Jérémie Decalf,[1] Sandrine Fernandes,[2] Randy Longman,[1,4] Mina Ahloulay,[2] Françoise Audat,[3] François Lefrerre,[3] Charles M. Rice,[4] Stanislas Pol,[2] and Matthew L. Albert[1,5]

[1]The Laboratory of Dendritic Cell Biology, Department of Immunology, Institut Pasteur, 75724 Paris, Cedex 15, France
[2]Institut National de la Santé et de la Recherche Médicale, U370, The Liver Unit, 75013 Paris, France
[3]The Division of Transfusion Medicine, Necker Hospital, 75015 Paris, Cedex 15, France
[4]The Rockefeller University, New York, NY 10065
[5]Institut National de la Santé et de la Recherche Médicale, U818, Paris, France

Plasmacytoid dendritic cells (pDCs) are the professional type I interferon (IFN)–producing cells, and upon activation they traffic to lymph organs, where they bridge innate and adaptive immunity. Using multianalyte profiling (MAP), we have mapped the key chemokines and cytokines produced in response to pDC activation, taking into consideration the role of autocrine IFN, as well as paracrine effects on other innate cells (e.g., monocytes and conventional DCs). Interestingly, we identify four distinct cytokine/chemokine loops initiated by Toll–like receptor engagement. Finally, we applied this analytic approach to the study of pDC activity in chronic hepatitis C patients. Based on the activation state of pDCs in fresh blood, the lack of agonistic activity of infectious virions, the production of a broad array of cytokines/chemokines once stimulated, and the direct effects of pDCs on other PBMCs, we conclude that the pDCs from hepatitis C virus (HCV)–infected individuals are fully functional and are, indeed, a viable drug target. In sum, this study provides insight into the use of MAP technology for characterizing cytokine networks, and highlights how a rare cell type integrates the activation of other inflammatory cells. Furthermore, this work will help evaluate the therapeutic application of pDC agonists in diseases such as chronic HCV infection.

CORRESPONDENCE
Matthew L. Albert:
albertm@pasteur.fr

Abbreviations used: cDC, conventional DC; HAU, hemagglutinating unit; HCV, hepatitis C virus; HEV, high endothelial venule; IFNAR, interferon α/β receptor; ICCS, intracellular cytokine stimulation; MAP, multianalyte profiling; NR, nonresponder; pDC, plasmacytoid DC; Rluc, Renilla luciferase; SVR, sustained virologic responder; TLR, Toll–like receptor.

Human plasmacytoid DCs (pDCs) are responsible for robust production of type I IFNs (1, 2). They express Toll-like receptor (TLR)-7 and -9, which recognize single-stranded RNA and double-stranded DNA, respectively (3–5). Upon stimulation, pDCs migrate to the T cell area of lymphoid organs via the high endothelial venules (HEVs), where they produce significant amounts of type I IFNs, suggesting a central role in pathogen recognition and the induction of innate immunity (6, 7). Increasing evidence indicates that pDCs are also critical in bridging innate and adaptive immune responses in the context of systemic viral or bacterial infections (1, 8). This is caused, in part, by the production

of IFNs, as well as their ability to participate in the recruitment of NK and activated T cells (9). More recently, it has been demonstrated that pDC-derived IFN supports conventional DCs (cDCs) in the priming of CD8^{+} T cells (8, 10). Although this adjuvant effect is now accepted, the precise cytokine and chemokine network that accounts for pDC's role in establishing an inflammatory microenvironment has been poorly characterized.

Taking advantage of multianalyte profiling (MAP) technology, we have performed an in-depth analysis of the cytokines and chemokines secreted by activated pDCs (1). Using both TLR-7 and -9 agonists, we confirmed what has been previously described concerning their secretory activity, and we identified additional inflammatory molecules directly expressed by pDCs. Specifically, we have used MAP for

characterization of the interactions between activated pDCs and other innate cells within the immune system. Interestingly, we identified four distinct cytokine loops by which pDCs contribute to the initiation of an inflammatory response: (a) molecules secreted by the pDC itself and independent of IFN production; (b) molecules secreted by the pDC and inhibited by paracrine IFN; (c) molecules secreted by the pDC and amplified by paracrine IFN; and (d) molecules not produced by pDCs, but triggered by paracrine IFN. Herein, we map each of the four mechanisms and show data with representative pDC-produced and –induced analytes.

Although pDC research has primarily focused on their ability to produce IFNs, and understandably so, as pDCs have been shown to produce 19 different type I IFNs, with this activity accounting for ~60% of the transcriptional activity (11), some studies have reported that pDCs secrete substantial amounts of other inflammatory molecules. Specifically, it has been shown that pDC stimulation results in the production of TNFα and IL-6, as well as the β chemokines CCL3 and CCL4 (9, 12–14). That said, many of these studies fail to demonstrate on a per cell basis that pDCs are the true source of the analyte in question. Furthermore, none of these studies used a systematic approach to define the extended array of molecules simultaneously produced by pDCs, nor has there been much consideration of the cells that are indirectly activated as a result of pDC-derived IFNs. Given the importance of pDCs in coordinating an inflammatory milieu, we believe our efforts offer critical information for understanding the programming of an antiviral or antibacterial response.

The analytic approach developed in this study lends itself to the evaluation of perturbations in the cytokine/chemokine network in different disease states. Several reports have indicated subversion of pDC function in hepatitis C virus (HCV) patients (15–18), and for this reason, we chose to define the functional status of pDCs in chronically infected individuals using MAP. This matter is of great importance, as it concerns not only the pathogenesis of HCV infection, but also the utility of novel therapeutic strategies based on targeting circulating pDCs. As shown here, by all measures, we find that pDCs from HCV-infected individuals are fully functional and are, indeed, a viable target for immunotherapy.

RESULTS
pDC activation results in the production of a broad array of proinflammatory molecules
To validate our stimulation protocols and define the experimental conditions used herein, we purified pDCs based on

BDCA-4 expression and stimulated them with TLR-7 or -9 agonists. As previously demonstrated, pDC activation resulted in high levels of IFNα production, expression of characteristic maturation markers, a shift in chemokine receptor expression, and an increased survival ex vivo (Fig. S1, available at http://www.jem.org/cgi/content/full/jem.20070814/DC1) (6, 10). We chose live influenza as an agonist, as it triggers rapid induction of IFN translation and protein accumulation such that it can be measured at an early time point by cytometric assays (Fig. S1 A and not depicted). Notably, pDCs respond to live influenza in a TLR-7–dependant manner (3, 19, 20). To further characterize the effects of TLR engagement and to define the role of pDCs in bridging innate and adaptive immunity, we used MAP technology to test the kinetics of production for 93 analytes using supernatants from stimulated pDCs. Using this initial screen, we defined a set of 12 molecules for this study (those not significantly produced by activated pDCs or by other cell types within the unfractionated PBMCs are listed in the Supplemental materials and methods). We chose a 20-h time point based on the observed kinetics of production for the different analytes (Fig. 1 A and not depicted). With this technology, we identified pDCs as being able to secrete a broad array of proinflammatory cytokines and chemokines. As shown, several cytokines (TNFα, IL-6, and IL-1Ra) and chemokines (CCL3, CCL4, IL-8, and CXCL10) are produced in response to influenza or CpG-2216 stimulation (Fig. 1 A). Although potential differences between influenza and CpG may reflect distinct pathogen-induced responses (Fig. S2), our interest was the definition of how activated pDCs initiate an inflammatory milieu.

For several of the key analytes, we tested whether pDCs are the true source by performing intracellular cytokine staining (Fig. 1 B). Indeed, this is the case for TNFα, CXCL10, and IL-8. Notably, pDCs do not produce CCL2, suggesting that the CCL2 found in some of the experiments (and possibly other analytes) is caused by a contaminating cell population. In fact, the effect of pDCs on other cell types is of great importance, and to assess which analytes are produced versus induced by activated pDCs, we performed MAP analysis on PBMCs and PBMCs depleted of pDCs (PBMCs-pDC). Because of the observation that influenza is stimulatory for other cell types within the PBMCs (unpublished data), we focused on CpG, as it is primarily acting on the pDCs. As expected, CpG-2216 triggered the production of IFNα, which was absent when pDCs were depleted (Fig. 1 C). Interestingly, the pattern of molecules produced does not follow the MAP of purified pDCs. We observe low amounts of TNF-α, CCL3,

Figure 1. TLR stimulation triggers pDCs to produce and induce a broad array of proinflammatory molecules. (A) 33,500 purified pDCs were cultured in 200 μl for 20 h with the indicated amount of FLU (hemagglutinating unit [HAU]/milliliter; black bars), CpG (micrograms/milliliter; gray bars), or media alone (ø; white bars). Supernatants were harvested and analyzed by Luminex. Data are expressed in nanograms/milliliter. The scale is indicated on the left. Data are the mean of duplicate wells, and each error bar indicates one SD. (B) To confirm the Luminex data, PBMCs were incubated for 5 h with media or 50 HAU/ml FLU. Cells were stained on the surface with pDC markers, fixed, permeabilized, and stained intracellularly for the indicated cytokine/chemokine. We looked at the cytokine/chemokine production on a per cell basis by gating on pDCs. (C) 10⁶ PBMCs (solid line) or PBMCs depleted of pDCs (PBMCs-pDCs; dashed line) were stimulated for 20 h with the indicated doses of CpG-2216 in 200 μl of culture media. Mean values of duplicate wells are presented. For A–C, results are representative of six independent experiments each, performed on a total of eight donors.

A

(20h stimulation)

B

C
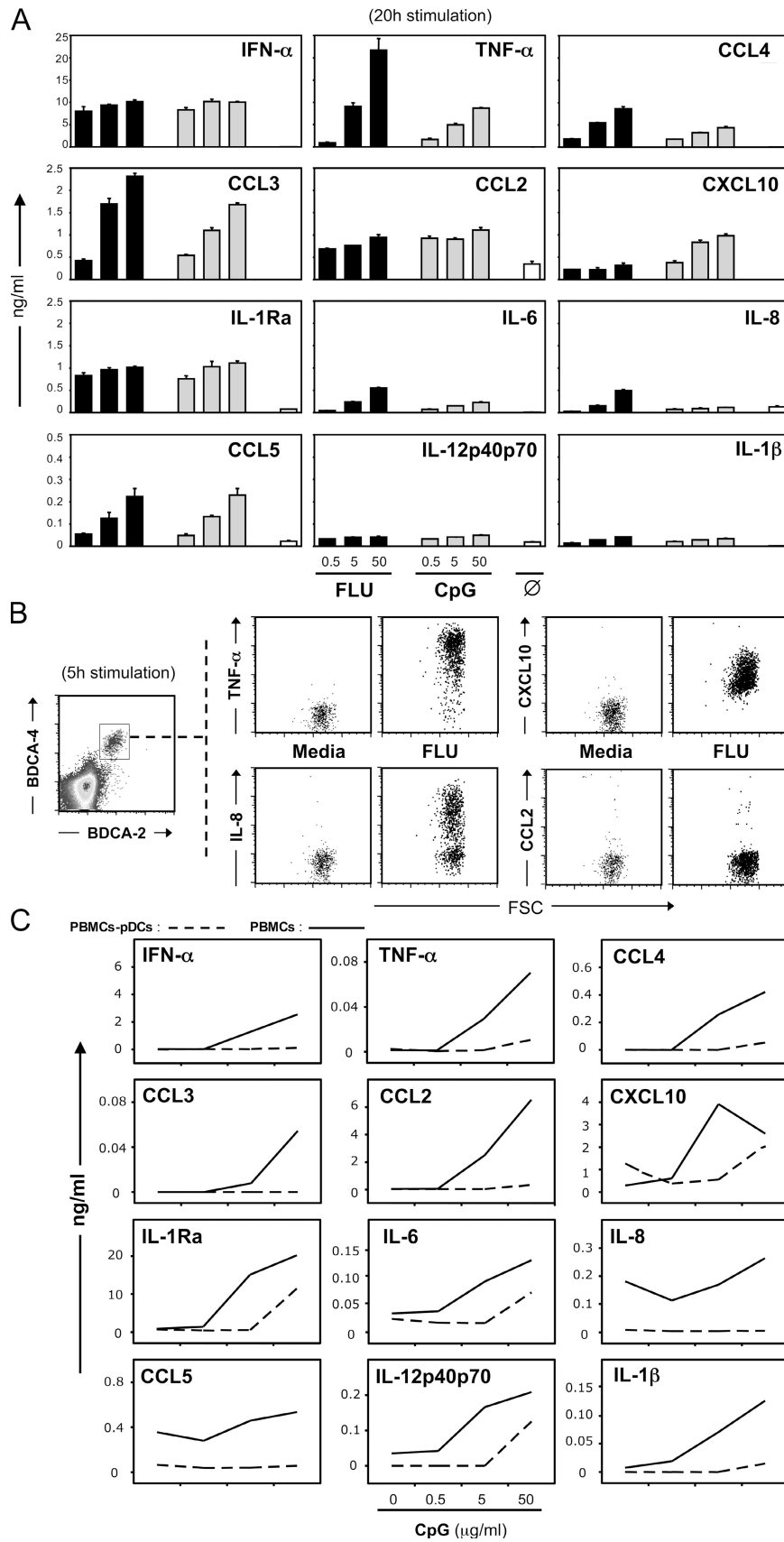
and CCL4 (Fig. 1 C), all of which were highly expressed by purified pDCs (Fig. 1). Notably, there were much higher levels of CCL2, CXCL10, and IL-1Ra produced by stimulated PBMCs than that observed from purified pDCs (Fig. 1 A, C), yet these three analytes are completely dependant on the presence of pDCs, as is evident from the absence of these molecules in the PBMCs-pDC condition. Although the dependence on pDCs is not too surprising, as we were stimulating the cells with a TLR-9 stimulus, these observations are important, as they suggest multiple mechanisms by which pDC activation influences chemokine and cytokine production. These results were also confirmed using FACS-purified pDCs ($n = 2$; unpublished data). In further dissecting the mechanisms by which pDCs initiate inflammatory responses, we defined four stimulation loops driven by TLR ligation and/or type I IFN production. We report on four molecules to illustrate these pathways: TNF-α, IL-8, CXCL10, and CCL2.

TLR engagement results in the production of TNFα independent of autocrine IFNα

TNFα is a pleiotropic inflammatory cytokine. It is produced by several cell types, but is predominantly secreted by macrophages in response to TLR-2 and -4 stimulation (21, 22). Depending, in part, on the TNF receptor expressed, cells may respond to cytokine stimulation by undergoing cell activation, cell division, or cell death (23). Although pDCs have been previously reported to produce TNFα, and some studies have explored its role in inhibiting IFNα, the influence of the IFNα cytokine loops on TNFα production has not been explored (24–26). Interestingly, pDCs exposed to influenza or CpG secrete robust levels of TNFα, producing on average 9.5×10^9 molecules of TNFα per pDC, which is calculated based on the molecular weight of TNFα and the number of cells used in the stimulation (Fig. 1). As shown, pDCs are directly producing TNFα (Fig. 1 B), and strikingly, they are one of the dominant sources of this cytokine when PBMCs are stimulated with influenza (Fig. 2 A, top plots). In contrast, when PBMCs are stimulated by LPS, the majority of responding cells are macrophage, and pDCs account for a negligible amount of the TNFα produced (Fig. 2 A, bottom plots). This is an important control, as it excluded the possibility that pDCs produce TNFα as a consequence of inflammation. However, as LPS does not trigger a strong IFNα response, it does not exclude the possibility that pDC-derived IFNα stimulates production of TNFα via an autocrine loop. To address this possibility, we stimulated purified pDCs with influenza in the presence of blocking antibodies specific for the interferon α/β receptor 2 (IFNAR2). No modulation of TNFα was observed (Fig. 2 B); moreover, pDCs stimulated with purified recombinant IFNα_{2b} did not stimulate TNFα production (Fig. 2 C). Together, these data indicate that engagement of TLR on pDCs results in the production of high levels of TNFα, and that this activation pathway is independent of its ability to produce type I IFNs (Fig. 2 D). We have also demonstrated that CCL3 follows this pattern of expression stimulation of pDCs (Fig. S3, available at http://www.jem.org/cgi/content/full/jem.20070814/DC1).
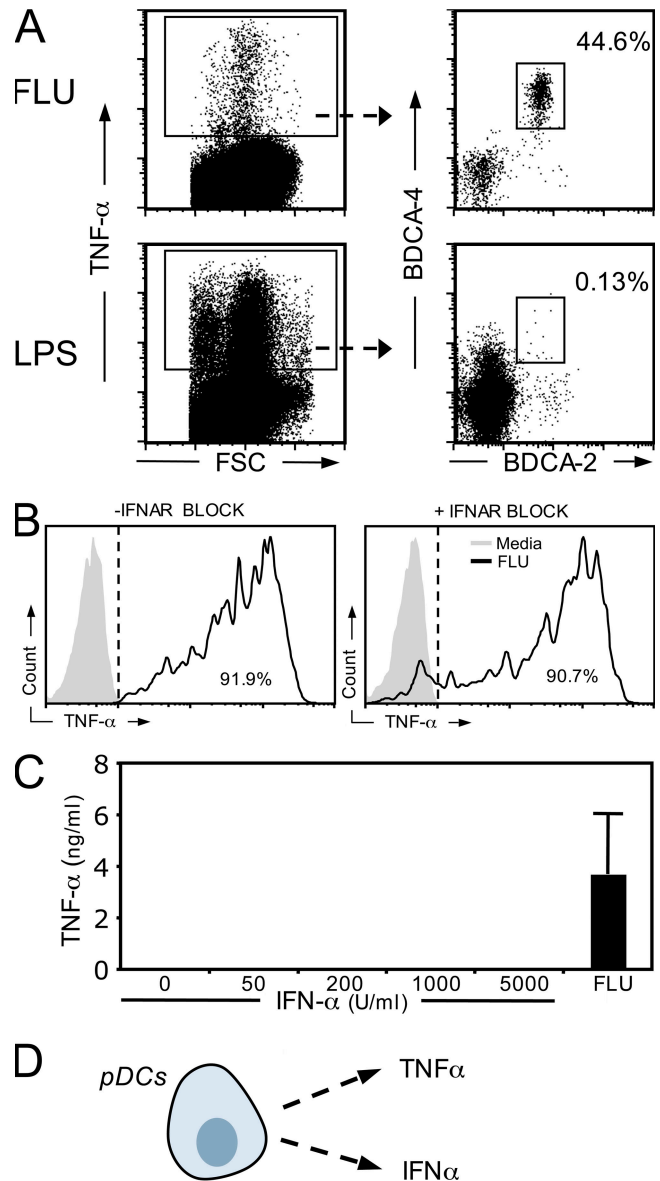
Figure 2. pDCs secrete robust amounts of TNFα in an IFNα–independent manner. (A) PBMCs were incubated for 5 h with 50 HAU/ml FLU or 10 μg/ml LPS, and brefeldin was added during the final 2 h 30 min. Unstimulated PBMCs were used to establish the gating of TNFα-positive cells (not depicted). (B) PBMCs were stimulated for 5 h with FLU ± anti-IFNAR2. ICCS and surface staining were again performed to evaluate TNFα production in stimulated pDCs. The histograms show TNFα levels in BDCA-2+ BDCA-4+ cells. (C) 22,000 purified pDCs were exposed to the indicated amount of rIFNα2. After 20-h incubation, supernatants were harvested and TNFα level was evaluated by Luminex. For each dataset, results are representative of two independent experiments. (D) A schematic representation of TNFα production by pDCs that are independent of the IFNα pathway.

pDC–derived IFN inhibits secretion of IL–8

IL–8, also called neutrophil-activating peptide-1 and CXCL8, is derived from several cell types in response to inflammatory stimuli. It functions as a chemoattractant and a stimulator of

angiogenesis (27, 28). As shown in Fig. 1, TLR stimuli induce IL-8 production in pDCs; although this may be expected given the broad tissue distribution of IL-8 production, pDCs are a unique case, as they also produce high amounts of IFNs, which are known to inhibit IL-8 production at the transcriptional level (29, 30). To test this cytokine loop, we again performed intracellular cytokine staining on activated pDCs in the presence or absence of anti-IFNAR2. Notably, the amount of IL-8 produced on a per cell basis was not significantly different when autocrine stimulation by type I IFNs was inhibited (Fig. 3 A). This result was confirmed by Luminex on supernatants of stimulated pDCs (Fig. 3 B). In contrast, the production of IL-8 by other PBMCs, monocytes in particular, increased dramatically in the presence of anti-IFNAR2 (Fig. 3 C). This could also be observed when we evaluated the levels of IL-8 in the supernatants of CpG-2216–stimulated PBMCs (Fig. 3 D). This was quite revealing, as in the absence of IFNAR blockade, IL-8 levels were undetectable; and it suggested that pDC-derived TNFα triggers IL-8 production (31). We confirmed this hypothesis by exposing PBMCs to recombinant TNFα in the presence of increasing amounts of IFNα (Fig. 3 E). As shown, TNFα has the ability to induce IL-8 production by whole PBMCs, but this effect is antagonized once IFNα is present in the media. As schematized in Fig. 3 F, we demonstrate that in respect to IL-8 induction, the following two opposing responses emerge from activated pDCs: induction by TNFα and its simultaneous inhibition by type I IFN.

CXCL10 is produced and induced by activated pDCs

IFNγ–inducible protein 10, now referred to as CXCL10, was first identified as an IFNγ–induced gene product produced by monocytes, endothelial cells, and fibroblasts (32). It has also been shown that type I IFNs and TNFα induces its production (33), and it was recently reported that pDCs are included among the cell types that can produce CXCL10 (34). Although our data support this result, with activated pDCs producing ~9 × 10⁸ molecules of CXCL10/cell (Fig. 1, A and B), an additional source of pDC-induced CXCL10 exists (Fig. 1 C). We first evaluated the production of CXCL10 by pDCs, and using anti-IFNAR2, we demonstrate that autocrine type I IFN amplifies CXCL10 mRNA expression in CpG-stimulated pDCs (Fig. 4 A). Next, we considered the effect of IFNα on other cell types. When rIFNα$_{2a}$ was added to PBMCs, we observed CXCL10 production by monocytes and cDCs (Fig. 4 B). We also evaluated CXCL10 production in lymphocytes and NK cells, but did not observe significant levels of CXCL10 production (unpublished data). Interestingly, pDCs were not stimulated to produce CXCL10 in response to IFNα alone, suggesting that synergy between TLR and IFNAR stimulation is required, accounting for the high production of CXCL10 by this cell type. To confirm that pDC-derived IFNs mediate release of CXCL10 after CpG stimulation, we monitored CXCL10 mRNA and protein in whole PBMCs in the presence of blocking antibodies, thus preventing the paracrine effects of type I IFNs (Fig. 4 C and not depicted).

As shown, pDC–derived IFNα is essential, as blocking IFNAR engagement or pDC-depletion from the PBMCs completely abrogated the expression of CXCL10. It should also be noted that after a short stimulation with CpG or IFNα, B cells do not secrete measurable levels of CXCL10 (Fig. 4 B and not depicted); however, after 20 h, it was indeed possible to detect direct activation of TLR-9 on B cells, resulting in the induction of CXCL10, confirming the results of Vollmer et al. (Fig. 4 D and not depicted) (35). These data illustrate the complex cytokine loops responsible for expression of CXCL10; moreover, it demonstrates that in some cell types, IFNα stimulation is sufficient for triggering CXCL10 (monocytes and cDCs), whereas in others (pDCs), IFNAR signaling serves as an amplifier of TLR activation, thus permitting the cell to achieve high levels of CXCL10 expression (Fig. 4 E). We have also demonstrated that CCL4 follows this pattern of expression after CpG stimulation of pDCs (Fig. S3).

CCL2 is not produced, but is robustly induced, by activated pDCs

Monocyte chemotactic protein-1, renamed CCL2, is a proinflammatory chemokine and plays a principal role in the recruitment of monocytes to sites of injury and inflammation (36). The current models suggest that CCL2 produced in the tissue may drain to the lymph node and facilitate trafficking of monocytes from the blood via the HEVs (37). We now demonstrate that activated pDC may be an additional trigger for CCL2 production. That said, the pDCs do not themselves produce CCL2 (Fig. 1 B); instead, activated pDCs induce production of CCL2 in PBMCs (Fig. 5 A). Based on experiments with recombinant IFNα$_{2a}$, we demonstrate that pDC-derived type I IFNs may serve as the stimulus for CCL2 production (Fig. 5 B), with the main cellular source being monocytes (Fig. 5 C and not depicted). These data illustrate a fourth mechanism by which pDCs may influence the inflammatory microenvironment of lymphoid organs (Fig. 5 D). We have also demonstrated that IL1RA follows this pattern of expression after CpG stimulation of pDCs (Fig. 1 C and not depicted).

pDCs in chronically infected HCV patients initiate a normal inflammatory network

We next applied our insight from the MAP of pDCs to the evaluation of HCV-infected patients. It is well recognized that subversion of pathways responsible for the stimulation of type I IFNs is a critical feature of HCV pathogenesis and, moreover, therapeutic IFNα$_2$ (given in combination with ribavirin) remains the standard of care for chronically infected patients (38). These observations led to attention being focused on the functional state of pDCs in patients who become chronically infected. There remains significant controversy in the field (15, 18, 39, 40), and arguably, some of the confusion stems from not fully addressing the complex role of pDCs in the establishment of an inflammatory milieu; instead, studies on this subject have simply relied on IFNα production as a measure of pDC activity.
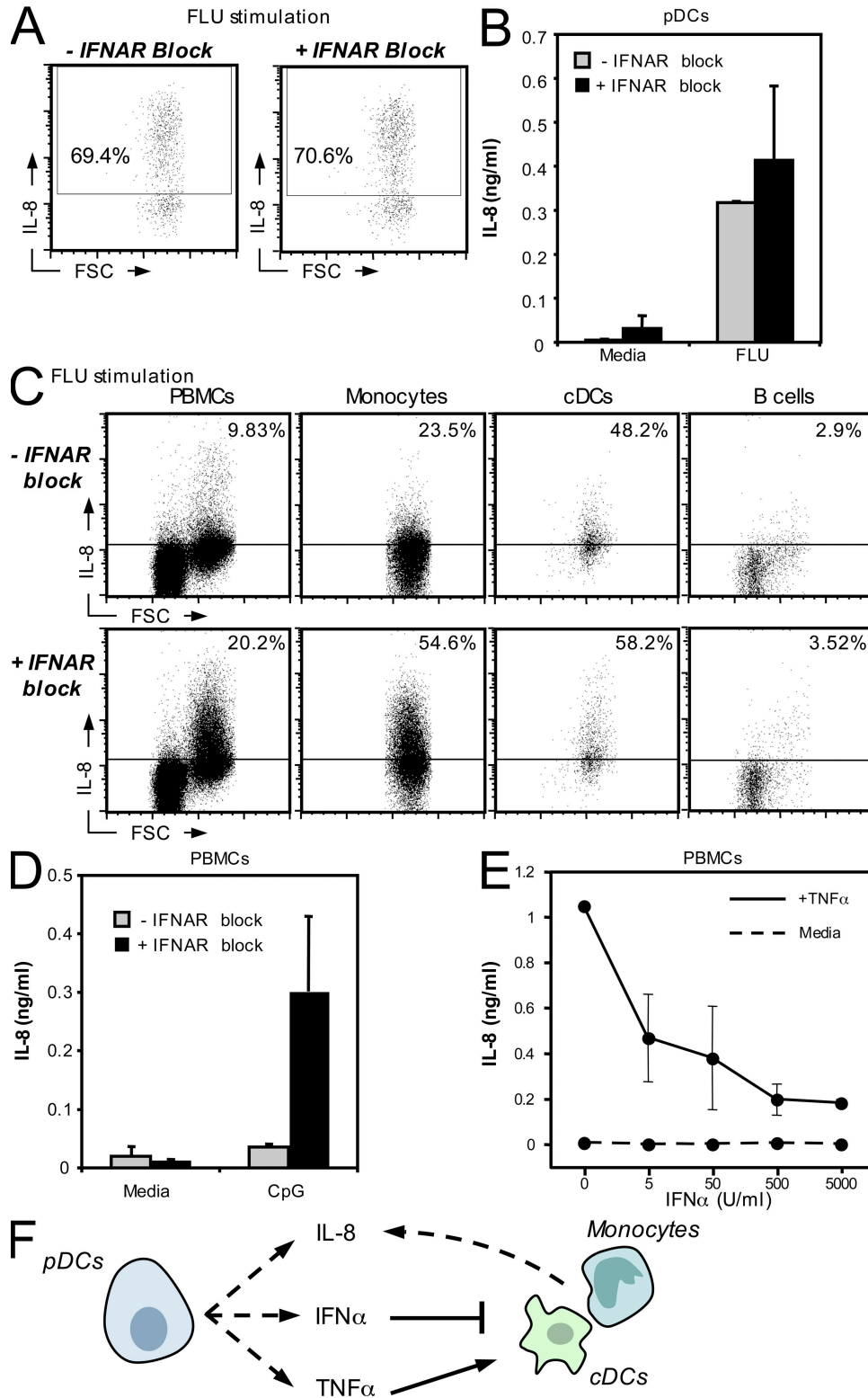
Figure 3. pDC–derived IFNα inhibits IL–8 production in monocytes and cDCs. (A) PBMCs were stimulated for 5 h with FLU ± anti-IFNAR2. ICCS and surface staining were performed to evaluate IL-8 production in stimulated pDCs. The plots show IL-8 levels in BDCA-2+ BDCA-4+ cells. (B) Purified pDCs were stimulated for 20 h with 50 HAU/ml FLU ± anti-IFNAR2, and supernatants were harvested and analyzed by Luminex. Data shown are the mean of results obtained from two donors. (C) PBMCs were stimulated for 5 h with 50 HAU/ml FLU ± anti-IFNAR2. ICCS and surface staining were performed to evaluate IL-8 production in monocytes (gated on CD14+ expression), cDCs (identified as BDCA-1+ CD19− cells), and B cells (gated on CD19+ expression). For each dataset, results are representative of two independent experiments. (D) 5 × 10^5 PBMCs were incubated for 5 h with 50 μg/ml
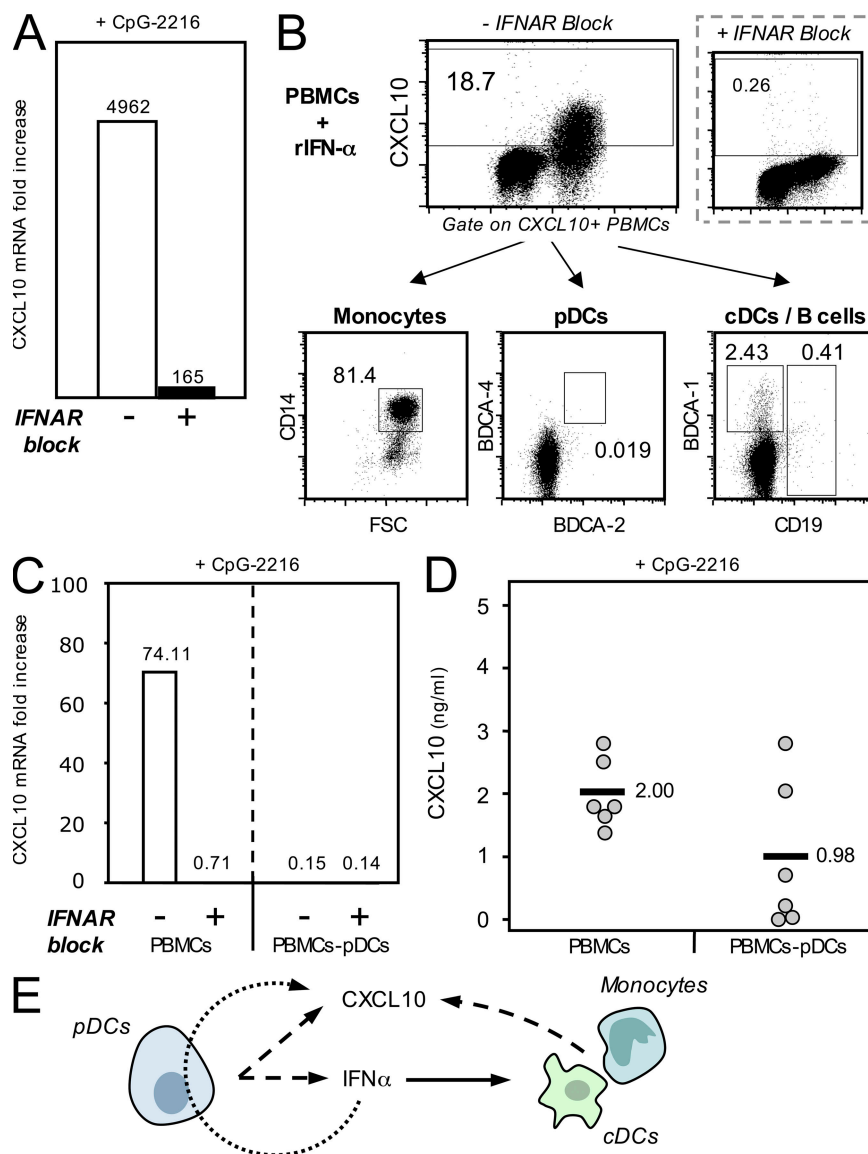
Figure 4. CXCL10 is amplified on pDCs and induced in PBMCs by pDC–derived IFNα. (A) Purified pDCs were stimulated for 3 h using 50 μg/ml CpG-2216. RNA were extracted and CXCL10 mRNA was evaluated by quantitative PCR, as detailed in the Materials and methods. (B) PBMCs were exposed for 5 h to recombinant IFNα2, and ICCS was performed. CXCL10 expression was evaluated for the different cell populations using lineage markers. As a negative control, we added anti-IFNAR2 antibodies to the culture wells. (C) PBMCs or PBMCs depleted of pDCs (PBMCs-pDCs) were exposed to 50 μg/ml CpG-2216 for 3 h in the presence of anti-IFNAR2. As in A, CXCL10 mRNA was evaluated by qPCR. (D) 10⁶ PBMCs and PBMCs-pDCs were stimulated for 20 h with 5 μg/ml CpG-2216 in 200 μl of culture media. Supernatants were harvested and CXCL10 levels were evaluated by Luminex. Each dot represents a unique donor ($n = 6$), and the bars indicate the mean value. (E) A schematic representation illustrating the direct and induced production of CXCL10 by activated pDCs.

We established a new cohort of patients who failed to respond to IFNα/ribavirin therapy (nonresponders [NRs]) and a control population of patients who are sustained virologic responders (SVRs; Table S1, available at http://www.jem .org/cgi/content/full/jem.20070814/DC1). Similar to our previous patient cohort, pDC enumeration in these patients indicated a slight reduction in the percentage of pDCs in NR HCV patients as compared with normal individuals

CpG-2216 ± anti-IFNAR2. Supernatants were harvested, and IL-8 levels were evaluated by Luminex. (E) 10⁶ PBMCs were cultured in the presence of 1 ng/ml rTNFα (solid line) or media alone (dashed line) in the presence of the increasing amounts of rIFNα. After 20 h, supernatants were harvested and IL-8 levels were evaluated by Luminex. Data show the average values obtained from experiments performed on two healthy donors. (F) A schematic representation illustrating the opposing effects of pDC-derived TNFα and IFNα on IL-8 production.

(unpublished data). In addition, we find lower numbers of pDCs in SVRs, suggesting that the presence of HCV in the plasma of patients is not directly responsible for the decrease in pDC number. We next assessed the phenotype of freshly isolated circulating pDCs as a direct measure of their activation state. pDCs were identified based on expression of BDCA-2 and -4 (Fig. S4 A). Gated cells were then analyzed

for their expression of defined maturation markers: CD80, CD86, CD83, HLA-DR, and the chemokine receptors CCR7 and CXCR3. In all patients tested, we observed resting-state levels of maturation markers (Fig. 6 A), offering evidence that circulating pDCs in SVR and NR HCV patients are in an inactive state. As a control that patient pDCs were able to undergo maturation, we stimulated cells and assessed patient
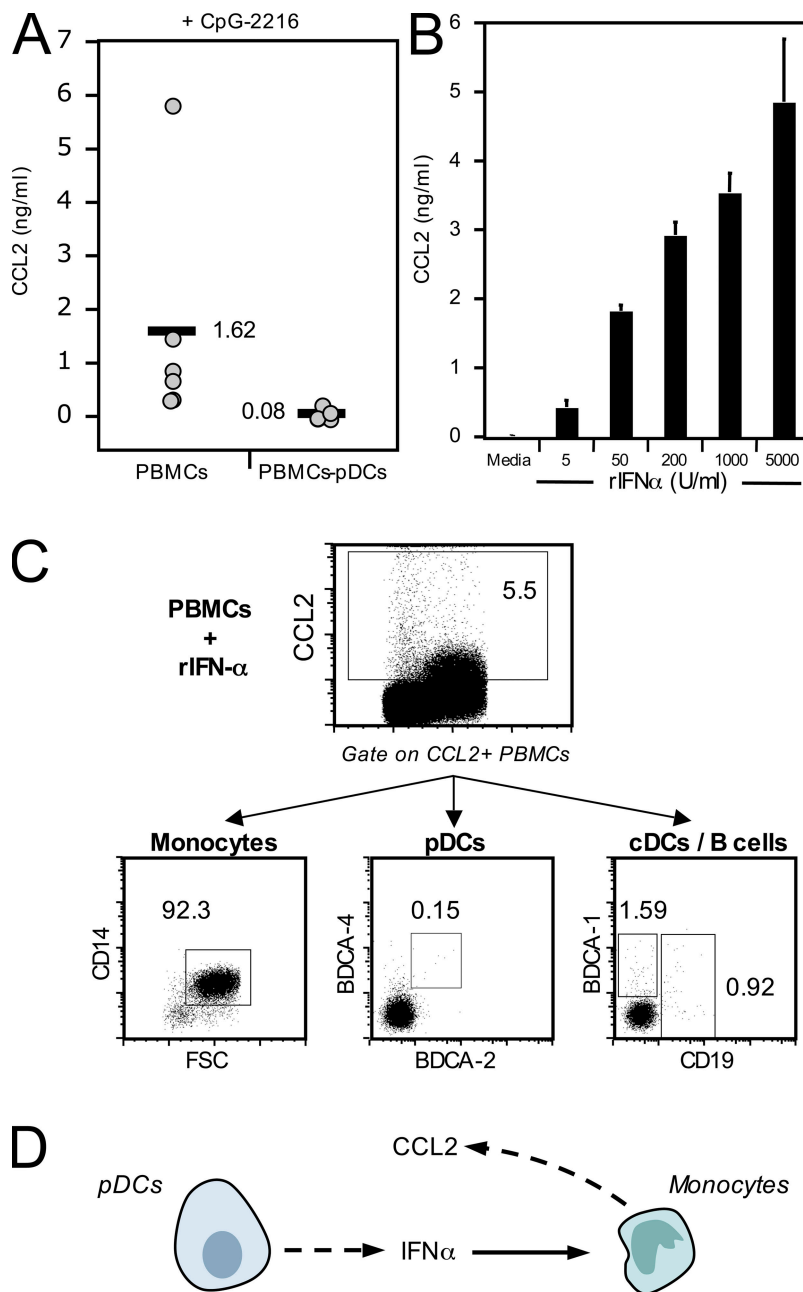

Figure 5. CCL2 is induced in PBMCs by pDC–derived IFNα. (A) 10^6 PBMCs and PBMCs depleted of pDCs (PBMCs-pDCs) were stimulated for 20 h using 5 μg/ml CpG-2216. Supernatants were harvested, and CCL2 protein levels were evaluated by Luminex. Each dot represents a unique donor ($n = 6$), and the bars indicate the mean value. (B) 10^6 PBMCs were exposed to the indicated amount or rIFNα2. After a 20-h incubation, supernatants were harvested and CCL2 levels were evaluated. Error bars indicate one SD. (C) PBMCs were exposed for 5 h to rIFNα2, and then ICCS was performed. CCL2 expression in a defined cell population was evaluated using lineage markers, including CD3, CD14, CD16, CD19, CD56, CD83, and BDCA-2. (D) A schematic representation illustrating the induction of CCL2 by pDC-derived IFNα. For B and C, data are representative of two independent experiments.
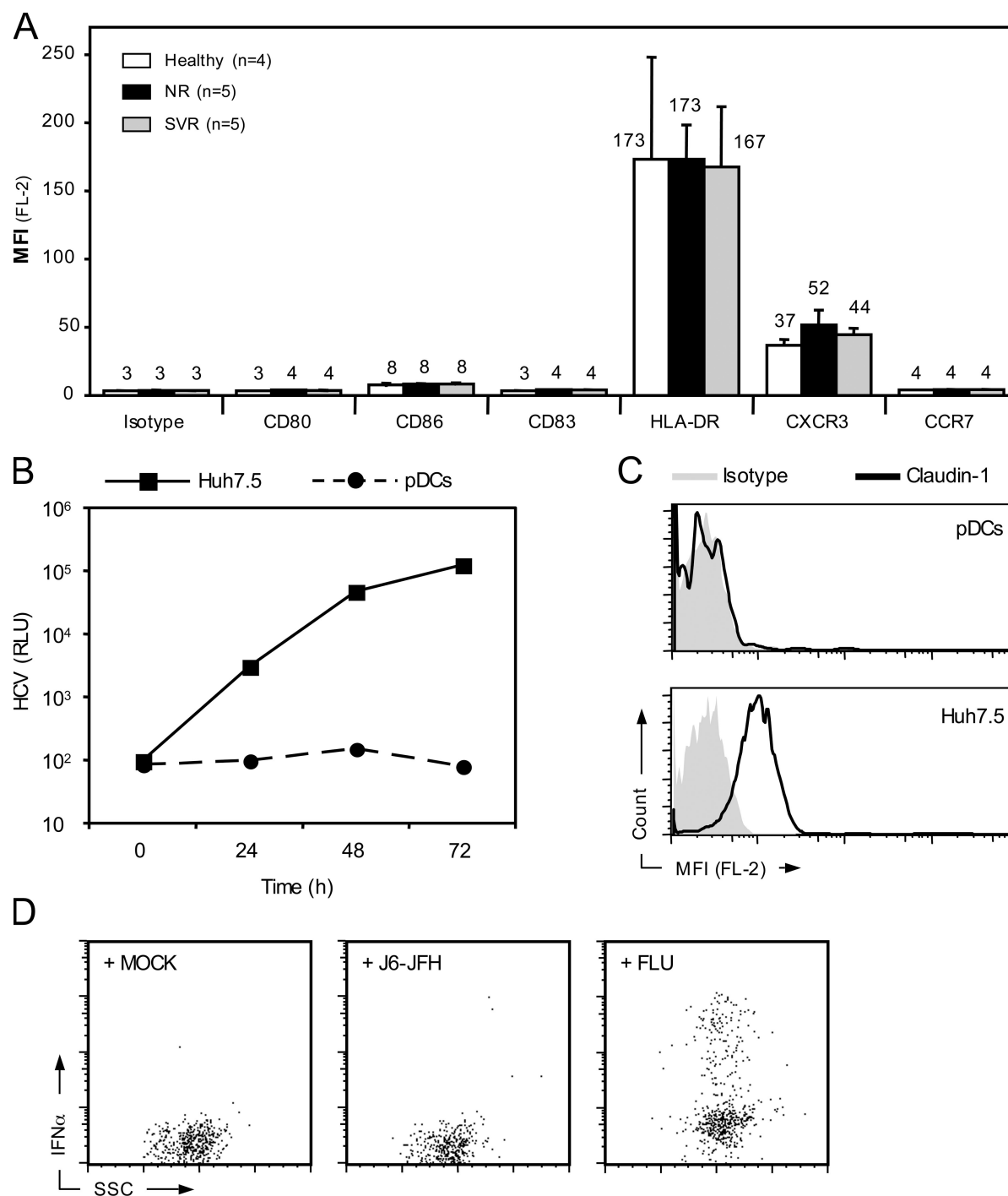
Figure 6. pDCs are not infected and not stimulated by replication–competent HCV. (A) pDCs were isolated from fresh PBMCs, and the phenotype was analyzed on samples from healthy control subjects ($n = 4$, white bars), NRs ($n = 5$, gray bars), and SVRs ($n = 5$, black bars). The bars represent the average mean fluorescence intensity of the FL-2 signal. (B) To directly evaluate infectability, 10^4 Huh7.5 cells or BDCA-4–purified pDCs were cultured in 96-well plates $\pm$ Rluc-J6-JF. After 12 h, cells were washed 3 times with PBS to remove free and membrane-bound viruses. Cells were replated in complete media, and this was considered as time = 0 h for the experiment. At 0, 24, 48, and 72 h, cells were monitored for luciferase activity. Recombinant IL-3 (10 ng/ml) was added in pDCs, and survival was confirmed by trypan blue exclusion at 72 h. Data shown are representative of two healthy donors. (C) Intracellular staining of claudin-1 was performed on Huh-7.5 cell line and freshly isolated PBMCs (from two healthy donors). Expression of claudin-1 by pDCs was evaluated by looking at BDCA-2+/BDCA-4+ cells within PBMCs. (D) 10^6 PBMCs were stimulated with media alone, influenza-A/PR8, or J6-JFH. After 5 h, intracellular cytokine staining was performed to evaluate IFNα production. pDCs were identified as BDCA-2+ BDCA-4+ cells within the PBMCs, and IFNα level on the gated cells is shown. Data are representative of experiments performed on PBMCs isolated from three healthy donors with two different viral preparations. These data were confirmed by IFNα Luminex in two additional donors (not depicted).
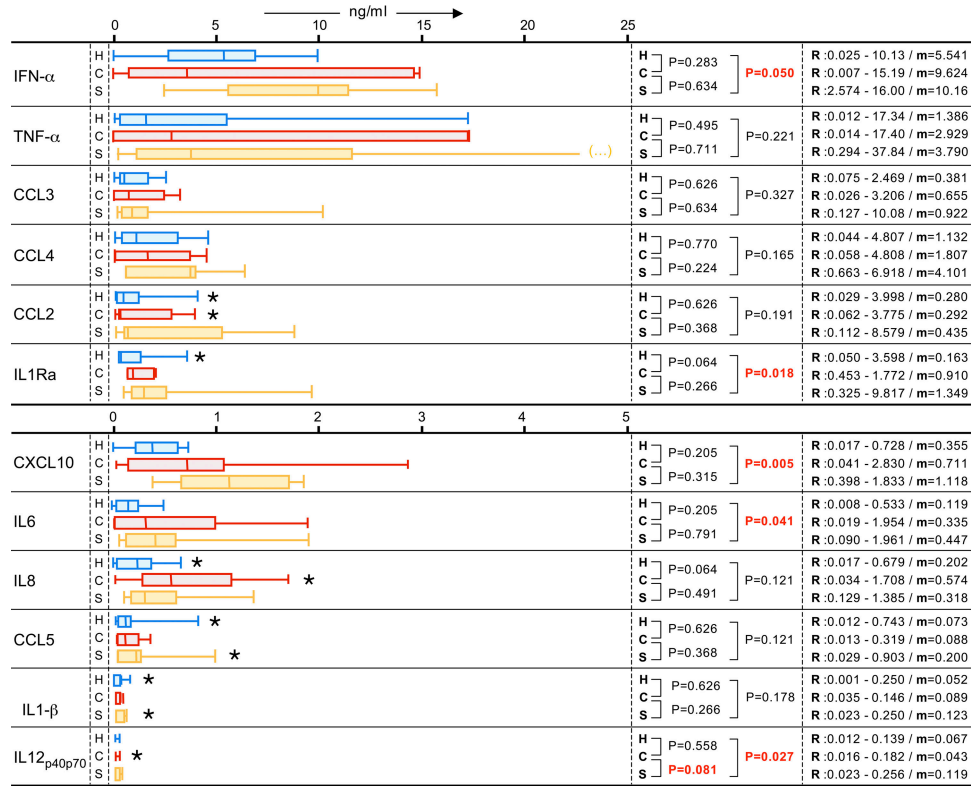
ng/ml →

Analyte		P values		R (min – max) / m (median)
IFN-α	H	P=0.283		R :0.025 - 10.13 / m=5.541
	C	P=0.634	P=0.050	R :0.007 - 15.19 / m=9.624
	S			R :2.574 - 16.00 / m=10.16
TNF-α	H	P=0.495		R :0.012 - 17.34 / m=1.386
	C	P=0.711	P=0.221	R :0.014 - 17.40 / m=2.929
	S			R :0.294 - 37.84 / m=3.790
CCL3	H	P=0.626		R :0.075 - 2.469 / m=0.381
	C	P=0.634	P=0.327	R :0.026 - 3.206 / m=0.655
	S			R :0.127 - 10.08 / m=0.922
CCL4	H	P=0.770		R :0.044 - 4.807 / m=1.132
	C	P=0.224	P=0.165	R :0.058 - 4.808 / m=1.807
	S			R :0.663 - 6.918 / m=4.101
CCL2	H	P=0.626		R :0.029 - 3.998 / m=0.280
	C	P=0.368	P=0.191	R :0.062 - 3.775 / m=0.292
	S			R :0.112 - 8.579 / m=0.435
IL1Ra	H	P=0.064		R :0.050 - 3.598 / m=0.163
	C	P=0.266	P=0.018	R :0.453 - 1.772 / m=0.910
	S			R :0.325 - 9.817 / m=1.349
CXCL10	H	P=0.205		R :0.017 - 0.728 / m=0.355
	C	P=0.315	P=0.005	R :0.041 - 2.830 / m=0.711
	S			R :0.398 - 1.833 / m=1.118
IL6	H	P=0.205		R :0.008 - 0.533 / m=0.119
	C	P=0.791	P=0.041	R :0.019 - 1.954 / m=0.335
	S			R :0.090 - 1.961 / m=0.447
IL8	H	P=0.064		R :0.017 - 0.679 / m=0.202
	C	P=0.491	P=0.121	R :0.034 - 1.708 / m=0.574
	S			R :0.129 - 1.385 / m=0.318
CCL5	H	P=0.626		R :0.012 - 0.743 / m=0.073
	C	P=0.368	P=0.121	R :0.013 - 0.319 / m=0.088
	S			R :0.029 - 0.903 / m=0.200
IL1-β	H	P=0.626		R :0.001 - 0.250 / m=0.052
	C	P=0.266	P=0.178	R :0.035 - 0.146 / m=0.089
	S			R :0.023 - 0.250 / m=0.123
IL12$_{p40p70}$	H	P=0.558		R :0.012 - 0.139 / m=0.067
	C	P=0.081	P=0.027	R :0.016 - 0.182 / m=0.043
	S			R :0.023 - 0.256 / m=0.119

Figure 7. Purified pDCs produce normal levels of TLR-9–induced cytokines and chemokines. pDCs (mean purity ∼90%) isolated from 10 healthy donors (H, blue bars), 7 NRs (red bars), and 9 SVRs (yellow bars) were stimulated with 5 µg/ml CpG-2216 for 20 h. Supernatants were harvested and MAP was performed using the Luminex technology. Data were analyzed with the OmniViz program, and Mann-Whitney tests were performed to obtain P values (statistically significant values, P ≤ 0.05, are shown in red). For each analyte, the range (R = min – max) and the median value (m) are indicated, expressed in nanograms/milliliter. Each stimulation was performed in duplicate, using 10^5 pDCs in 200 µl of culture media. * indicates the measured analytes that were not statistically different from unstimulated cells (not depicted; Mann-Whitney tests, P ≥ 0.05).

pDC phenotype. As shown in the representative plots, the pDCs from all three cohorts underwent a rapid maturation looking at several surface molecules (Fig. S4 B, solid lines).

The lack of pDC activation in patients with high viral titer would suggest that HCV was neither infecting nor stimulating pDCs. To directly test this supposition, we used the replication-competent chimeric HCV, J6-JFH (41–43). First, we evaluated direct infection of the pDC using a J6-JFH strain engineered to express cytoplasmic luciferase (44). Although the hepatocellular line Huh-7.5 was readily infected, pDCs did not show any luciferase activity. Importantly, in this experiment, IL-3 was added to the pDC cultures to ensure survival over the 72-h time course (Fig. 6 B). In addition, we evaluated pDC's expression of the recently identified HCV coreceptor claudin-1 (45). Whereas the HCV-permissive cell line Huh-7.5 expresses high levels of claudin-1, expression on pDCs was undetectable. These data support our observation that pDCs are not infected, but it does not exclude the possibility that viral engagement of pDCs might result in pDC activation.

To address this question, we tested if J6-JFH exposure might induce pDCs to produce IFNα. Strikingly, no IFNα was produced in response to live, replication-competent HCV

(Fig. 6 D and not depicted). This observation was confirmed by exposing pDCs derived from healthy individuals to primary isolate HCV in the presence of antiserum (unpublished data). As a positive control in our experiments, we used influenza A/PR8 as a pDC agonist. Finally, we tested if exposure to JFH-1J6 might abrogate pDC's ability to respond to TLR stimuli. In coculture experiments, we find no evidence that live HCV virions alter a pDC's ability to produce IFNα secondary to CpG and live influenza stimulation (unpublished data). We also evaluated if high viral titer plasma from patients could stimulate purified pDCs (Fig. S5, available at http://www.jem.org/cgi/content/full/jem.20070814/DC1). These plasma contain free viruses, as well as anti-E2 antibodies that can lead to formation of antibody–virus complexes (46). These data indicate that pDCs do not secret IFNα in the presence of high viral titer plasma, suggesting that indirect entry of the virus, going through Fc receptors, does not lead to pDC activation. Together, these data support the absence of infection and the presence of quiescent pDCs within chronically infected HCV patients.

We next applied MAP to define the inflammatory network triggered by the activation of purified patient pDCs. Data were analyzed using a bioinformatics tool developed by

OmniViz, and patient data are represented as whisker-box plots, showing absolute amounts of the respective cytokine or chemokine (Figs. 7). To the right of each plot, the range (R) and median (M) value is reported. The Mann-Whitney test was used to determine statistical differences between each pair of patient cohorts: healthy (H) versus NR chronically infected patients (N); healthy (H) versus SVRs (S); and NRs (N) versus SVRs (S). Each P value is reported, and those values ≤ 0.05 are shown in red. Overall, there is a striking similarity between the patient cohorts in respect to their pDC activity. For several analytes, however, we did observe statistically significant differences. Interestingly, in each of these instances, the HCV patients were producing higher levels of the respective analyte on a per pDC basis. In the case of IFNα, CXCL10, and IL-6 production, we detected statistically significant differences in stimulated pDCs isolated from SVR than from healthy individuals. To determine if any of these differences were relevant to the pDCs ability to provoke an inflammatory cascade and to take into account the observed differences in absolute pDC number (unpublished data), we next defined the MAP of unfractionated PBMCs stimulated with CpG-2216 (Fig. 8). Notably, there were no statistically significant differences across the three cohorts,

and we observed the expected patterns of expression for all cytokines/chemokines. We conclude that the pDCs in HCV patients are normal across several independent criteria. Indeed, they are functionally active in regard to their ability to produce a broad spectrum of proinflammatory molecules, thus permitting the initiation of an appropriate inflammatory network.

DISCUSSION

pDCs coordinate the production of four distinct chemokine and cytokine loops

Using MAP, we have characterized the network of chemokines and cytokines produced upon pDC activation. Interestingly, this technology lends itself to working with rare cell populations such as pDCs, as simultaneous measurements can be achieved using small amounts of cell supernatant. In addition, through the use of recombinant cytokines and blocking antibodies to cytokine receptors, it has been possible to provide a detailed analysis of what occurs when pDCs are activated by TLR-7 or -9 agonists. We find that although pDCs represent a small percentage of the PBMCs, they trigger a remarkable cascade of chemokine and cytokine production. We define four distinct cytokine loops that together help
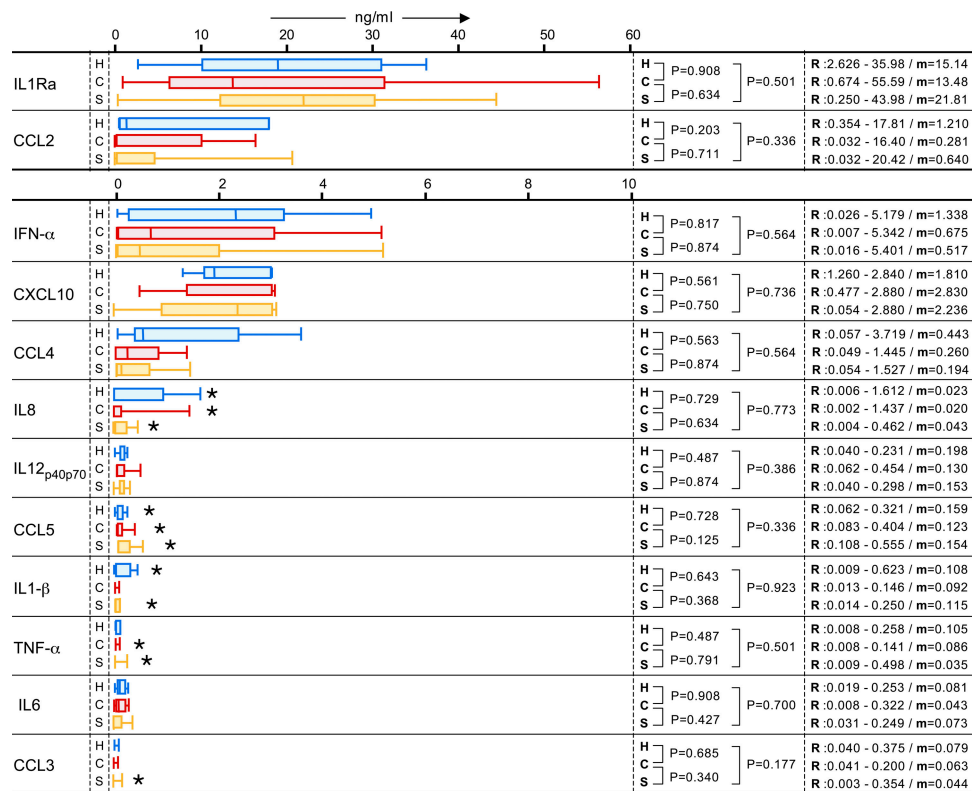

Figure 8. The pDC–mediated inflammatory network is intact in chronically infected HCV patients. Freshly isolated PBMCs from 8 healthy donors (H, blue bars), 7 NRs (red bars), and 9 SVRs (S, yellow bars) were stimulated with 5 μg/ml CpG-2216 for 20 h. Supernatants were harvested, and MAP was performed using the Luminex technology. Data were analyzed with the OmniViz program, and Mann-Whitney tests were performed to obtain P values (statistically significant values, P ≤ 0.05, are shown in red). For each analyte, the range (R = min − max) and the median value (m) are indicated, expressed in nanograms/milliliter. Each stimulation was performed in duplicate using 10^6 pDCs in 200 μl of culture media. * indicates the measured analytes that were not statistically different from unstimulated cells (not depicted; Mann-Whitney tests, P ≥ 0.05).

establish the proinflammatory response initiated by pDC activation (Fig. S6, available at http://www.jem.org/cgi/content/full/jem.20070814/DC1). Specifically, we have characterized these cytokine loops in respect to the pDCs innate ability to produce type I interferons. In the first, activated pDCs secrete factors such as TNFα and CCL3 in a manner that is triggered by TLR engagement and independent of IFNAR stimulation (Fig. 2 and Fig. S3). In the second, IL-8 is the only molecule we identified that follows a second pattern of expression; it is secreted by pDCs in response to TLR engagement, but its production is inhibited by IFNAR signaling (Fig. 3). Interestingly, pDCs are refractory to the inhibitory effects of IFN, suggesting that TLR-7– and -9–induced IL-8 production follows a different signaling pathway from TNFα-mediated IL-8 stimulation (Fig. 3, A and B, and not depicted). The third class of molecules is secreted by pDCs in response to TLR engagement, with their expression being enhanced by autocrine IFN. In the case of CXCL10 and CCL4, pDC-derived IFN may also induce other cell types to produce these chemokines in a manner that is apparently independent of direct TLR stimulation (Fig. 4 and Fig. S3). In the fourth cytokine loop, illustrated by CCL2 and also true for IL1Ra, IL1β, and IL-12p70, the pDCs do not produce, but instead induce, the production of these molecules by other cell types (Fig. 5 and not depicted). These results suggest a coordinated set of events that support recruitment of defined cells and the production of inflammatory analytes for the initiation of an afferent immune response.

Although we have not directly evaluated the signaling pathways that mediate these four cytokine loops, and there exists the caveat of extrapolating from mouse experiments that primarily rely on embryonic fibroblasts derived from knockout animals, published data, indeed, supports such a demarcation of events upon pDC activation. We predict that the IFN-independent production of TNFα and CCL3 is mediated by an IFN regulatory factor-5–regulated gene induction program (47). This is predicated on the observation that $Irf5^{-/-}$ hematopoietic cells respond to CpG by producing type I IFNs, but fail to secrete TNFα in addition to other proinflammatory cytokines. Inhibition of IL-8 has been carefully characterized, and studies of the human *IL-8* promoter demonstrate that IFNα/β suppresses its NF-κB site–mediated transcription (30). As IL-8 mediates neutrophil migration, its inhibition might be an important hallmark of pDC-initiated inflammation in the lymph organs. Concerning the third signaling loop, the small but significant amount of IFNAR-independent CXCL10 is likely a result of TLR-induced phosphorylation of IFN regulatory factor-3, which acts as a homodimer and induces the transcription of *CXCL10* (48, 49). The autocrine and paracrine amplification could be explained by the activation of IFN-stimulated gene factor 3, which will act on the ISRE within the promoter of *CXCL10* (33). Finally, it is also the IFN-stimulated gene factor that could account for the induction of CCL2, IL1Ra, IL-1β, and IL-12p70 in cells that are predisposed toward producing these molecules (11, 50). Clearly, additional modulators of gene transcription (and possibly translation) exert their control and help define on a molecular level the regulation of these four cytokine loops.

A viable drug target in chronically infected HCV patients

There are nearly 200 million HCV-infected individuals worldwide, posing a significant public health risk (51). Approximately 30% of people infected with HCV resolve infection, whereas 70% progress to chronic infection. Given the recent observations concerning the role of type I IFN in facilitating cDCs to prime CD8+ T cells, it has been considered that HCV inhibits pDC function, thereby limiting endogenous IFN production. Indeed, there have been several studies that report evidence for impaired DC subsets in chronically infected patients (17, 52, 53). As it is difficult to reconcile these data with the observation that individuals chronically infected with HCV are not immunocompromised and that, in fact, they have high levels of endogenous IFN (54), we performed an in-depth evaluation of the phenotypic measures and functional activity of patient pDCs compared with normal controls. It is important to note that prior studies have limited their analysis to the pDC's ability to produce IFNα/β. In this study, we have considered the pDC in the context of its inflammatory network and demonstrate that there is neither a defect in circulating pDCs nor in the ability of pDCs to engage other PBMCs for the establishment of a chemokine and cytokine network.

In addition to immunologic measures of pDC function, we considered the direct effects of replication-competent virus on freshly isolated pDCs. We report no direct infection and find no evidence for HCV virions resulting in pDC activation (Fig. 6, B and D). Notably, these experiments were performed using a highly sensitive measure of infection, as the recombinant viruses were engineered to express renilla luciferase (Rluc). We also demonstrate that pDCs do not express the HCV receptor claudin-1. Finally, we demonstrate evidence that virus–antibody immune complexes present in HCV plasma do not result in pDC activation (Fig. S5). Given the lack of an intrinsic defect in chronically infected HCV patient pDCs, and the ability of circulating cells to respond appropriately to TLR stimulation, it is exciting to consider the use of pDC agonists as an alternative therapeutic intervention.

The current standard of care for chronic HCV infection is a 1-yr course of pegylated IFNα (PEG-IFN) and ribavirin (55). The PEG-IFN is administered subcutaneously and results in a blood level of 10–25 ng/ml of type I IFNα/β. Although this therapy results in ~50% viral clearance, there are significant adverse effects, including mental health problems (e.g., irritability, depression, and anxiety), leukopenia, thrombopenia, and changes in vision. New therapeutics are desperately needed and pDC agonists are an exciting option for two reasons (56–58). First, it facilitates delivery of the IFN stimulation to the lymph node microenvironment. This is achieved by harnessing the biology of activated pDCs, which up-regulate CCR7 and traffic to the site of T cell priming. In this

way, it offers a second potential benefit. By concentrating the IFNα production to the lymphoid organs, it may be possible to achieve similar activity with lower systemic levels of IFNα. Thus, the stimulation of the hypothalamic–pituitary–adrenal axis may be less significant, helping to avoid some of the more severe side effects of therapy, such as mood disorders.

In sum, we provide an in-depth characterization of the first integrated map of the pDC chemokine/cytokine network, and conclude that the pDCs generated from patients with chronic HCV infection are phenotypically and functionally normal. This work also establishes a solid foundation for pDC immunotherapy, where the pDC itself would serve as the drug target, in turn releasing IFNα/β into the lymph node microenvironment and facilitating the activation of adaptive immune responses. We expect that the analytic approach developed in this study will be of use in the evaluation of perturbations in the cytokine/chemokine network in different disease states.

MATERIALS AND METHODS

Cell preparation and isolation. Buffy coat were obtained from the Établissement Français du Sang. PBMCs were separated from granulocytes, erythrocytes, and platelets using Ficoll-Paque PLUS (GE Healthcare). Plasmacytoid DCs were isolated from 500×10^6 PBMCs using the anti–BDCA-4 magnetic beads (Miltenyi Biotec) following the manufacturer's protocol. Three populations were obtained: PBMCs, enriched pDCs (90–95% purity), and PBMCs depleted of pDCs (PBMCs-pDCs, <0.01% pDCs). In all experiments, freshly isolated cells were used.

Cell stimulation. Freshly isolated cells were resuspended in RPMI (Cambrex) that had been supplemented with 10% FCS (Eurobio). Number of cells and time of stimulation are indicated in the figure legends of each experiment. All stimulations were performed in 96-well flat-bottom plates (BD Biosciences) in a fixed volume of 200 μl of media. Cells were stimulated with influenza virus strain A/PR8/1976 (Charles River Laboratories), LPS (serotype O55:5; Sigma-Aldrich), or CpG-2216 (5′-GGGGGACGATC-GTCGGGGGG-3′; Eurogentec). Recombinant IFNα$_2$ (Sigma-Aldrich) and TNFα (R&D Systems) were reconstituted in PBS and stored at −80°C. Mouse monoclonal antibodies specific for human IFNAR2 (PBL biomedical) were used at 5 μg/ml and added simultaneously with the pDC agonist used. For intracellular cytokine staining experiments, cells were stimulated for 5 h with live influenza virus, and GolgiPlug (BD Biosciences) was added during the last 2 h.

Supernatant analysis. After stimulation, supernatants were harvested and conserved at −80°C for further analysis. Chemokines and cytokines were measured by Luminex (12 plex kits; Biosource) following the manufacturer's instructions. In brief, 50 μl of supernatant or standard was incubated with antibody-linked beads for 2 h, washed twice with wash solution, and incubated for 1 h with biotinylated secondary antibodies. A final incubation of 30 min with streptavidin-PE preceded the acquisition on the Luminex 100IS. At least 100 events were acquired for each analyte. Values above or below the standard curves were replaced by the lowest or the highest concentrations measured. Where applicable, two-tailed nonparametric comparisons (Mann-Whitney *U* test) were performed to calculate P values. Statistical analyses were performed with the OmniViz program.

Flow cytometric analysis. Stimulated cells were transferred to 96-well round-bottom plates, washed once, and resuspended in 100 μl of FACS buffer (PBS, 1% FCS, and 1% pooled human sera). In intracellular cytokine stimulation (ICCS) experiments, surface lineage markers were used to identify pDCs (BDCA-2 FITC and BDCA-4 APC; Miltenyi Biotec), B cells and cDCs (CD19 FITC [BD Bioscience]; BDCA-1 APC [Miltenyi Biotec]), and monocytes (CD14 FITC; BD Bioscience) within stimulated PBMCs. Mouse anti–human CXCL10, IL-8, TNFα (BD Biosciences), and CCL2 (eBioscience) antibodies were directly conjugated to PE. IFNα staining was performed in two steps. First, mouse anti-IFNα (PBL Biomedical) was used, followed by staining with a secondary antibody conjugated to PE (goat anti–mouse IgGs; Biosource). For PE-conjugated antibodies, cells were surface labeled, fixed, permeabilized, and stained for intracellular cytokine production. For IFNα detection, cells were fixed and permeabilized first so that the secondary antibody would not have the possibility to cross-react with surface-bound antibodies. pDC phenotype analysis (Fig. 6 A) was performed by staining for pDC surface lineage markers (BDCA-2 FITC, BDCA-4 APC; Miltenyi Biotec) associated with the desired phenotype marker in FL-2 channel (isotype PE, CD80 PE, CD86 PE, CD83 PE, HLA-DR PE, CXCR3 PE, and CCR7 PE; all purchased from BD Biosciences). Cells were incubated for 20 h at 4°C and analyzed by FACS, as indicated in the figure legend. Intracellular staining of claudin-1 was performed on fresh PBMCs (note, the available antibody recognizes an intracellular domain of the protein). Mouse anti–claudin-1 (Zymed Laboratories) was incubated for 20 h, followed by a secondary antibody conjugated to PE. Staining was followed by antibodies specific for surface markers BDCA-2/-4, thus allowing us to determine claudin-1 expression in pDCs.

Quantitative analysis of mRNA in stimulated cells. Total RNA from 3-h-stimulated cells were extracted using Trizol (Invitrogen), and cDNA was synthesized from 1–2 μg RNA using oligo-dT (Roche) and Superscript reverse transcriptase (Invitrogen) according to the manufacturers' instructions. Quantitative real-time PCR was performed using the TaqMan gene expression assays technology (Applied Biosystems) for CXCL10 (Hs00171042_m1), CCL2 (Hs00234142_m1), and CCL4 (Hs00237011_m1). GAPDH was used as a housekeeping gene to normalize mRNA expression. The ratio of gene of interest versus housekeeping gene was calculated according to the following formula: ratio = 2 − dCt (dCT = mean Ct gene − mean Ct housekeeping). The mRNA fold increase was calculated as the ratio between mRNA in stimulated cells and mRNA in unstimulated cells. The reactions were run on a PTC200 equipped with a Chromo4 detector (MJ Research). The analyses were performed with Opticon Monitor software version 2.03 (MJ Research). All the measures were performed in duplicate and validated when the difference in threshold cycle (Ct) between the 2 measures was <0.3.

Patient cohort. The study protocol RBM 03–59 was approved by the Institut National de la Santé et de la Recherche Médicale clinical investigation department and received ethical approval from the ethical committee of Necker Hospital (Consultative Committee for Protection of Persons in Biomedical Research). 22 HCV patients had chronic infection as defined by anti-HCV antibodies and HCV RNA positivity for a period of time >6 mo. They all had biopsy-proven chronic hepatitis related to a genotype 1 infection. 21/22 patients were treated by a combination of pegylated interferon and ribavirin for at least 3 mo (Table S1); 12 were SVRs and 10 were NRs. SVRs were defined as individuals absent of HCV RNA for >6 mo after termination of therapy. NRs had viral persistence and liver injury. Samples were collected by leukapheresis for 17/22 patients, and from whole blood donations for 5/22 individuals.

Preparation of Rluc-J6-JFH and luciferase assay. J6-JFH and J6-JFH–expressing Rluc were generated as previously described (44). Regarding the luciferase-expressing virus, the Rluc gene was inserted between the P7 and NS2 proteins of the J6-JFH chimeric virus, allowing for a cytoplasmic expression of the enzyme during viral replication. Viral stocks were prepared by harvesting the supernatants of Huh7.5 cells infected with J6-JFH or Rluc-J6-JFH and storing them at −80°C.

Luciferase assay. Cells exposed to Rluc-J6-JFH were washed twice with PBS and lysed with Renilla lysis buffer (Promega). Lysates were harvested

and frozen at −80°C for further analysis. Frozen samples were thawed, and 10 μl of samples were mixed with luciferase assay substrate (Promega). Luciferase activity was measured using a luminometer (Lumat LB 9507; Berthold Technologies).

Online supplemental material. Table S1 shows the characteristics of the HCV patients included in the study. Fig. S1 shows that pDCs mature and secrete IFNα in response to TLR ligands. Fig. S2 shows the production of proinflammatory chemokines and cytokines by purified pDCs. Fig. S3 shows the differential regulation of CCL3 and CCL4 production. Fig. S4 shows that pDCs isolated from chronic HCV patients undergo a normal maturation when stimulated in vitro. Fig. S5 shows that purified healthy pDCs do not produce IFNα when they are exposed to high viral titer HCV plasma. Fig. S6 is a schematic summarizing the four different loops of regulation described in the study. The online version of this article is available at http://www.jem.org/cgi/content/full/jem.20070814/DC1.

REFERENCES

1. Liu, Y.J. 2005. IPC: professional type 1 interferon-producing cells and plasmacytoid dendritic cell precursors. *Annu. Rev. Immunol.* 23:275–306.

2. Colonna, M., G. Trinchieri, and Y.J. Liu. 2004. Plasmacytoid dendritic cells in immunity. *Nat. Immunol.* 5:1219–1226.

3. Diebold, S.S., T. Kaisho, H. Hemmi, S. Akira, and C. Reis e Sousa. 2004. Innate antiviral responses by means of TLR7-mediated recognition of single-stranded RNA. *Science.* 303:1529–1531.

4. Lund, J.M., L. Alexopoulou, A. Sato, M. Karow, N.C. Adams, N.W. Gale, A. Iwasaki, and R.A. Flavell. 2004. Recognition of single-stranded RNA viruses by Toll-like receptor 7. *Proc. Natl. Acad. Sci. USA.* 101:5598–5603.

5. Hemmi, H., O. Takeuchi, T. Kawai, T. Kaisho, S. Sato, H. Sanjo, M. Matsumoto, K. Hoshino, H. Wagner, K. Takeda, and S. Akira. 2000. A Toll-like receptor recognizes bacterial DNA. *Nature.* 408:740–745.

6. Cella, M., F. Facchetti, A. Lanzavecchia, and M. Colonna. 2000. Plasmacytoid dendritic cells activated by influenza virus and CD40L drive a potent TH1 polarization. *Nat. Immunol.* 1:305–310.

7. Asselin-Paturel, C., A. Boonstra, M. Dalod, I. Durand, N. Yessaad, C. Dezutter-Dambuyant, A. Vicari, A. O'Garra, C. Biron, F. Briere, and G. Trinchieri. 2001. Mouse type I IFN–producing cells are immature APCs with plasmacytoid morphology. *Nat. Immunol.* 2:1144–1150.

8. Yoneyama, H., K. Matsuno, E. Toda, T. Nishiwaki, N. Matsuo, A. Nakano, S. Narumi, B. Lu, C. Gerard, S. Ishikawa, and K. Matsushima. 2005. Plasmacytoid DCs help lymph node DCs to induce anti-HSV CTLs. *J. Exp. Med.* 202:425–435.

9. Megjugorac, N.J., H.A. Young, S.B. Amrute, S.L. Olshalsky, and P. Fitzgerald-Bocarsly. 2004. Virally stimulated plasmacytoid dendritic cells produce chemokines and induce migration of T and NK cells. *J. Leukoc. Biol.* 75:504–514.

10. Asselin-Paturel, C., and G. Trinchieri. 2005. Production of type I interferons: plasmacytoid dendritic cells and beyond. *J. Exp. Med.* 202:461–465.

11. Ito, T., H. Kanzler, O. Duramad, W. Cao, and Y.J. Liu. 2006. Specialization, kinetics, and repertoire of type 1 interferon responses by human plasmacytoid predendritic cells. *Blood.* 107:2423–2431.

12. Piqueras, B., J. Connolly, H. Freitas, A.K. Palucka, and J. Banchereau. 2006. Upon viral exposure, myeloid and plasmacytoid dendritic cells produce 3 waves of distinct chemokines to recruit immune effectors. *Blood.* 107:2613–2618.

13. Penna, G., M. Vulcano, A. Roncari, F. Facchetti, S. Sozzani, and L. Adorini. 2002. Cutting edge: differential chemokine production by myeloid and plasmacytoid dendritic cells. *J. Immunol.* 169:6673–6676.

14. Jego, G., A.K. Palucka, J.P. Blanck, C. Chalouni, V. Pascual, and J. Banchereau. 2003. Plasmacytoid dendritic cells induce plasma cell differentiation through type I interferon and interleukin 6. *Immunity.* 19:225–234.

15. Kanto, T., M. Inoue, M. Miyazaki, I. Itose, H. Miyatake, M. Sakakibara, T. Yakushijin, A. Kaimori, C. Oki, N. Hiramatsu, et al. 2006. Impaired function of dendritic cells circulating in patients infected with hepatitis C virus who have persistently normal alanine aminotransferase levels. *Intervirology.* 49:58–63.

16. Szabo, G., and A. Dolganiuc. 2005. Subversion of plasmacytoid and myeloid dendritic cell functions in chronic HCV infection. *Immunobiology.* 210:237–247.

17. Kanto, T., M. Inoue, H. Miyatake, A. Sato, M. Sakakibara, T. Yakushijin, C. Oki, I. Itose, N. Hiramatsu, T. Takehara, et al. 2004. Reduced numbers and impaired ability of myeloid and plasmacytoid dendritic cells to polarize T helper cells in chronic hepatitis C virus infection. *J. Infect. Dis.* 190:1919–1926.

18. Murakami, H., S.M. Akbar, H. Matsui, N. Horiike, and M. Onji. 2004. Decreased interferon-alpha production and impaired T helper 1 polarization by dendritic cells from patients with chronic hepatitis C. *Clin. Exp. Immunol.* 137:559–565.

19. Schulz, O., S.S. Diebold, M. Chen, T.I. Naslund, M.A. Nolte, L. Alexopoulou, Y.T. Azuma, R.A. Flavell, P. Liljestrom, and C. Reis e Sousa. 2005. Toll-like receptor 3 promotes cross-priming to virus-infected cells. *Nature.* 433:887–892.

20. Kato, H., O. Takeuchi, S. Sato, M. Yoneyama, M. Yamamoto, K. Matsui, S. Uematsu, A. Jung, T. Kawai, K.J. Ishii, et al. 2006. Differential roles of MDA5 and RIG-I helicases in the recognition of RNA viruses. *Nature.* 441:101–105.

21. Medzhitov, R., P. Preston-Hurlburt, E. Kopp, A. Stadlen, C. Chen, S. Ghosh, and C.A. Janeway Jr. 1998. MyD88 is an adaptor protein in the hToll/IL-1 receptor family signaling pathways. *Mol. Cell.* 2:253–258.

22. Qureshi, S.T., L. Lariviere, G. Leveque, S. Clermont, K.J. Moore, P. Gros, and D. Malo. 1999. Endotoxin-tolerant mice have mutations in Toll-like receptor 4 (*Tlr4*). *J. Exp. Med.* 189:615–625.

23. Ware, C.F. 2005. Network communications: lymphotoxins, LIGHT, and TNF. *Annu. Rev. Immunol.* 23:787–819.

24. Kadowaki, N., S. Antonenko, J.Y. Lau, and Y.J. Liu. 2000. Natural interferon α/β-producing cells link innate and adaptive immunity. *J. Exp. Med.* 192:219–226.

25. Gary-Gouy, H., P. Lebon, and A.H. Dalloul. 2002. Type I interferon production by plasmacytoid dendritic cells and monocytes is triggered by viruses, but the level of production is controlled by distinct cytokines. *J. Interferon Cytokine Res.* 22:653–659.

26. Palucka, A.K., J.P. Blanck, L. Bennett, V. Pascual, and J. Banchereau. 2005. Cross-regulation of TNF and IFN-alpha in autoimmune diseases. *Proc. Natl. Acad. Sci. USA.* 102:3372–3377.

27. Walz, A., R. Burgener, B. Car, M. Baggiolini, S.L. Kunkel, and R.M. Strieter. 1991. Structure and neutrophil-activating properties of a novel inflammatory peptide (ENA-78) with homology to interleukin 8. *J. Exp. Med.* 174:1355–1362.

28. Baggiolini, M., A. Walz, and S.L. Kunkel. 1989. Neutrophil-activating peptide-1/interleukin 8, a novel cytokine that activates neutrophils. *J. Clin. Invest.* 84:1045–1049.

29. Aman, M.J., G. Rudolf, J. Goldschmitt, W.E. Aulitzky, C. Lam, C. Huber, and C. Peschel. 1993. Type-I interferons are potent inhibitors of interleukin-8 production in hematopoietic and bone marrow stromal cells. *Blood.* 82:2371–2378.

30. Oliveira, I.C., N. Mukaida, K. Matsushima, and J. Vilcek. 1994. Transcriptional inhibition of the interleukin-8 gene by interferon is mediated by the NF-kappa B site. *Mol. Cell. Biol.* 14:5300–5308.

31. Matsushima, K., and J.J. Oppenheim. 1989. Interleukin 8 and MCAF: novel inflammatory cytokines inducible by IL 1 and TNF. *Cytokine.* 1:2–13.

32. Luster, A.D., and J.V. Ravetch. 1987. Biochemical characterization of a γ interferon-inducible cytokine (IP-10). *J. Exp. Med.* 166:1084–1097.

33. Ohmori, Y., and T.A. Hamilton. 1993. Cooperative interaction between interferon (IFN) stimulus response element and kappa B sequence motifs controls IFN gamma- and lipopolysaccharide-stimulated transcription from the murine IP-10 promoter. *J. Biol. Chem.* 268:6677–6688.

34. Krug, A., A. Towarowski, S. Britsch, S. Rothenfusser, V. Hornung, R. Bals, T. Giese, H. Engelmann, S. Endres, A.M. Krieg, and G. Hartmann. 2001. Toll-like receptor expression reveals CpG DNA as a unique microbial stimulus for plasmacytoid dendritic cells which synergizes with CD40 ligand to induce high amounts of IL-12. *Eur. J. Immunol.* 31:3026–3037.

35. Vollmer, J., M. Jurk, U. Samulowitz, G. Lipford, A. Forsbach, M. Wullner, S. Tluk, H. Hartmann, A. Kritzler, C. Muller, et al. 2004. CpG oligodeoxynucleotides stimulate IFN-gamma-inducible protein-10 production in human B cells. *J. Endotoxin Res.* 10:431–438.

36. Yoshimura, T., N. Yuhki, S.K. Moore, E. Appella, M.I. Lerman, and E.J. Leonard. 1989. Human monocyte chemoattractant protein-1 (MCP-1). Full-length cDNA cloning, expression in mitogen-stimulated blood mononuclear leukocytes, and sequence similarity to mouse competence gene JE. *FEBS Lett.* 244:487–493.

37. Palframan, R.T., S. Jung, G. Cheng, W. Weninger, Y. Luo, M. Dorf, D.R. Littman, B.J. Rollins, H. Zweerink, A. Rot, and U.H. von Andrian. 2001. Inflammatory chemokine transport and presentation in HEV: a remote control mechanism for monocyte recruitment to lymph nodes in inflamed tissues. *J. Exp. Med.* 194:1361–1373.

38. Feld, J.J., and J.H. Hoofnagle. 2005. Mechanism of action of interferon and ribavirin in treatment of hepatitis C. *Nature.* 436:967–972.

39. Piccioli, D., S. Tavarini, S. Nuti, P. Colombatto, M. Brunetto, F. Bonino, P. Ciccorossi, F. Zorat, G. Pozzato, C. Comar, et al. 2005. Comparable functions of plasmacytoid and monocyte-derived dendritic cells in chronic hepatitis C patients and healthy donors. *J. Hepatol.* 42:61–67.

40. Longman, R.S., A.H. Talal, I.M. Jacobson, C.M. Rice, and M.L. Albert. 2005. Normal functional capacity in circulating myeloid and plasmacytoid dendritic cells in patients with chronic hepatitis C. *J. Infect. Dis.* 192:497–503.

41. Zhong, J., P. Gastaminza, G. Cheng, S. Kapadia, T. Kato, D.R. Burton, S.F. Wieland, S.L. Uprichard, T. Wakita, and F.V. Chisari. 2005. Robust hepatitis C virus infection in vitro. *Proc. Natl. Acad. Sci. USA.* 102:9294–9299.

42. Lindenbach, B.D., M.J. Evans, A.J. Syder, B. Wolk, T.L. Tellinghuisen, C.C. Liu, T. Maruyama, R.O. Hynes, D.R. Burton, J.A. McKeating, and C.M. Rice. 2005. Complete replication of hepatitis C virus in cell culture. *Science.* 309:623–626.

43. Wakita, T., T. Pietschmann, T. Kato, T. Date, M. Miyamoto, Z. Zhao, K. Murthy, A. Habermann, H.G. Krausslich, M. Mizokami, et al. 2005. Production of infectious hepatitis C virus in tissue culture from a cloned viral genome. *Nat. Med.* 11:791–796.

44. Tscherne, D.M., C.T. Jones, M.J. Evans, B.D. Lindenbach, J.A. McKeating, and C.M. Rice. 2006. Time- and temperature-dependent activation of hepatitis C virus for low-pH-triggered entry. *J. Virol.* 80:1734–1741.

45. Evans, M.J., T. von Hahn, D.M. Tscherne, A.J. Syder, M. Panis, B. Wolk, T. Hatziioannou, J.A. McKeating, P.D. Bieniasz, and C.M. Rice. 2007. Claudin-1 is a hepatitis C virus co-receptor required for a late step in entry. *Nature.* 446:801–805.

46. Nattermann, J., A.M. Schneiders, L. Leifeld, B. Langhans, M. Schulz, G. Inchauspe, B. Matz, H.H. Brackmann, M. Houghton, T. Sauerbruch, and U. Spengler. 2005. Serum antibodies against the hepatitis C virus E2 protein mediate antibody-dependent cellular cytotoxicity (ADCC). *J. Hepatol.* 42:499–504.

47. Takaoka, A., H. Yanai, S. Kondo, G. Duncan, H. Negishi, T. Mizutani, S. Kano, K. Honda, Y. Ohba, T.W. Mak, and T. Taniguchi. 2005. Integral role of IRF-5 in the gene induction programme activated by Toll-like receptors. *Nature.* 434:243–249.

48. Nakaya, T., M. Sato, N. Hata, M. Asagiri, H. Suemori, S. Noguchi, N. Tanaka, and T. Taniguchi. 2001. Gene induction pathways mediated by distinct IRFs during viral infection. *Biochem. Biophys. Res. Commun.* 283:1150–1156.

49. Honda, K., and T. Taniguchi. 2006. IRFs: master regulators of signalling by Toll-like receptors and cytosolic pattern-recognition receptors. *Nat. Rev. Immunol.* 6:644–658.

50. Matikainen, S., J. Pirhonen, M. Miettinen, A. Lehtonen, C. Govenius-Vintola, T. Sareneva, and I. Julkunen. 2000. Influenza A and sendai viruses induce differential chemokine gene expression and transcription factor activation in human macrophages. *Virology.* 276:138–147.

51. De Francesco, R., and G. Migliaccio. 2005. Challenges and successes in developing new therapies for hepatitis C. *Nature.* 436:953–960.

52. Auffermann-Gretzinger, S., E.B. Keeffe, and S. Levy. 2001. Impaired dendritic cell maturation in patients with chronic, but not resolved, hepatitis C virus infection. *Blood.* 97:3171–3176.

53. Bain, C., A. Fatmi, F. Zoulim, J.P. Zarski, C. Trepo, and G. Inchauspe. 2001. Impaired allostimulatory function of dendritic cells in chronic hepatitis C infection. *Gastroenterology.* 120:512–524.

54. Mihm, S., M. Frese, V. Meier, P. Wietzke-Braun, J.G. Scharf, R. Bartenschlager, and G. Ramadori. 2004. Interferon type I gene expression in chronic hepatitis C. *Lab. Invest.* 84:1148–1159.

55. Fried, M.W., M.L. Shiffman, K.R. Reddy, C. Smith, G. Marinos, F.L. Goncales Jr., D. Haussinger, M. Diago, G. Carosi, D. Dhumeaux, et al. 2002. Peginterferon alfa-2a plus ribavirin for chronic hepatitis C virus infection. *N. Engl. J. Med.* 347:975–982.

56. Lee, J., C.C. Wu, K.J. Lee, T.H. Chuang, K. Katakura, Y.T. Liu, M. Chan, R. Tawatao, M. Chung, C. Shen, et al. 2006. Activation of anti-hepatitis C virus responses via Toll-like receptor 7. *Proc. Natl. Acad. Sci. USA.* 103:1828–1833.

57. Horsmans, Y., T. Berg, J.P. Desager, T. Mueller, E. Schott, S.P. Fletcher, K.R. Steffy, L.A. Bauman, B.M. Kerr, and D.R. Averett. 2005. Isatoribine, an agonist of TLR7, reduces plasma virus concentration in chronic hepatitis C infection. *Hepatology.* 42:724–731.

58. Klinman, D.M. 2004. Immunotherapeutic uses of CpG oligodeoxynucleotides. *Nat. Rev. Immunol.* 4:249–258.